Acta Geotechnica (2021) 16:595–611
https://doi.org/10.1007/s11440-020-01045-0

RESEARCH PAPER

Study of hidden factors affecting the mechanical behavior of soil–rock mixtures based on abstraction idea

Hui Dong[1] · Bocheng Peng[1] · Qian-Feng Gao[2] · Yin Hu[1] · Xiuzi Jiang[1]

Received: 16 May 2019 / Accepted: 20 July 2020 / Published online: 30 July 2020

Abstract

Because of spatial variability and complex compositions, the mechanical test results of natural soil–rock mixtures (SRMs) are often discrete and lack reproducibility, which has greatly restricted the practical application of the experimental findings. The objective of this study was to examine the general mechanical behavior of SRMs under the influences of some hidden factors (e.g., structural parameters, parent rock type and weathering degree). To that end, the abstraction idea was adopted to prepare purified SRM samples. Large-scale triaxial tests were performed on these purified materials. On this basis, the influences of three structural parameters on the mechanical behavior of SRMs were studied. Moreover, the relationship between the shear strength and parent rock type and that between the shear strength and the spatial distribution of rock blocks were quantified. Some additional intrinsic behavior was distinguished from individual experimental phenomena through the comparative analysis of the test data in this study and those reported in the literature. The results show that the hidden factors had significant influences on the mechanical behavior of SRMs. A greater saturated uniaxial compressive strength of rock blocks generally led to a larger shear strength of SRMs. According to the significance of their influences on the shear strength parameters of SRMs, the structural parameters are ordered as: the gradation of rock blocks, the initial dry density of sample and the spatial distribution of rock blocks. The deformation and failure feature of SRMs were considerably affected by the spatial distribution of rock blocks and shear rate. And the shear strength parameters of SRMs were mainly influenced by the content of grains between 40 and 60 mm. The findings of this study would provide useful guidance for engineering practice.

Keywords Abstraction idea · Mechanical behavior · Parent rock · Soil-rock mixture · Structure

1 Introduction

Soil-rock mixtures (SRMs) are a type of inhomogeneous, discontinuous and loose geomaterial composed of both soil matrix (e.g., clay, silt and sand) and rock blocks (e.g., gravel and stone) [13, 18]. SRMs are extensively distributed in nature and also widely used as filling materials in road engineering and hydropower engineering [13, 27, 32, 51]. The large-scale direct shear test, large-scale triaxial test and in situ test are common methods for measuring the mechanical properties of SRMs [20, 34, 45, 49]. Because of complex material compositions, the mechanical behavior of SRMs is considerably distinct from those of "soil" and "rock" alone [45]. For this reason, the determination of the mechanical behavior of SRMs has been a very challenging task and has received great attention from researchers and engineers.

Plenty of previous work has shown evidences that structural parameters (e.g., initial dry density, gradation, and spatial distribution of rock blocks) have influences on the mechanical behavior of SRMs [18, 43]. Specifically, Miller and Sowers [28] stated that the cohesion and angle of internal friction changed rapidly as the stone content increased from 67 to 74%, and the angle of internal friction had no significant change when the stone content exceeded 74%. And Cen [4] reported that the cohesion reduced while

✉ Qian-Feng Gao
qianfeng.gao@csust.edu.cn

[1] Hunan Key Laboratory of Geomechanics and Engineering Safety, Xiangtan University, Xiangtan 411105, China

[2] School of Traffic & Transportation Engineering, Changsha University of Science & Technology, Changsha 410114, China

the angle of internal friction increased with increasing stone content, which was consistent with the results of Lindquist and Goodman [24]. However, Medley [26] found that the angle of internal friction increased considerably as the stone content varied from 24 to 42%; Coli et al. [8] found that the cohesion went down the fastest as the stone content increased from 17 to 26% and then remained almost stable as the stone content further increased. Meanwhile, Chen and Zhang [6] reported that as the gravel content increased from 30 to 80%, the cohesion and angle of internal friction of silty sand improved by gravel increased nonlinearly and linearly, respectively. The above results indicate that no general consensus has been reached on how the gradation affects the mechanical behavior, particularly the cohesion, of SRMs. Moreover, some researchers quantified the structure of SRMs using photography or computed tomography (CT) and then analyzed the mechanical behavior of SRMs by numerical simulations (De Frias Lopez et al. [11], Gong et al. [14], Zhou et al. [52], Meng et al. [27], Li et al. [23] and Xu et al. [46]). Among them, Li et al. [23] and Xu et al. [46] reported that the spatial distribution of rock blocks affects the stress distribution and the development of shear zones. Nevertheless, SRMs are usually regarded as homogeneous media, and the spatial distribution of rock blocks in SRMs is rarely considered in laboratory tests.

In addition, many experimental studies have shown different mechanical behavior of SRMs due to the difference in parent rock types. For instance, Alonso et al. [2] reported that the shear strength of Pancrudo slate rockfill was always less than that of Garraf limestone rockfill under the same test condition. Kalender et al. [21] performed uniaxial and triaxial compression tests on unwelded bimrocks and bimsoils. The authors stated that the cohesion decreased while both the angle of internal friction and Young's modulus increased with increasing rock block content. The study conducted by Huang et al. [18] on clay–dolomite mixtures demonstrated that there was no obvious correlation between the cohesion and stone content and the angle of internal friction increased linearly with increasing stone content. The test methods used by Huang et al. [18] and Kalender et al. [21] were both large-scale triaxial tests, and the materials used by them were both SRMs but the findings obtained by them were quite different. This is probably resulted from the parent rock differences of their materials. Rock blocks with different parent rock types have distinct deformability and uniaxial compressive strengths [33, 37]; thus, some rock blocks are brittle and easy to break while others behave in a more ductile manner. One can imagine that this will lead to different mechanical behavior of SRMs [36]. However, there was no specific quantitative study on how the variation of parent rock type affects the mechanical behavior of SRMs to date.

Since the influences of structural parameters and parent rock type are often easily neglected by engineers, they can be termed hidden factors (compared with the widely concerned factors including water content, confining pressure, sample size, etc.) to the mechanical behavior of SRMs. As a matter of fact, these hidden factors make it difficult to identify whether the experimental findings are individual phenomena or intrinsic behavior, which has highly restricted the practical application of the experimental findings. Thus, the simplification of the problem is needed in order to reveal the general and intrinsic mechanical behavior of SRMs. Shen [35] proposed to use the abstraction idea (which means to strengthen the most intrinsic features while weakening the non-intrinsic features) to deal with such issues. Following that idea, when examining the influence of parent rock types on the mechanical behavior, only the parent rock type varies between different samples while the other features (e.g., structural parameters) of all samples are unified strictly, artificially. This helps to improve the reproducibility of test results and reveal the intrinsic behavior of SRMs.

The purpose of this study was to examine the general mechanical behavior of SRMs affected by various hidden factors. A series of large-scale triaxial tests were performed on the purified SRM samples, which were reconstituted from the soil matrix of known mineral compositions and the rock blocks of given parent rock types and weathering degrees. On this basis, the influences of three sample-scale structural parameters (i.e., initial dry density of sample, gradation of rock blocks and spatial distribution of rock blocks) on the mechanical behavior of SRMs were studied. Meanwhile, the effects of the spatial distribution of rock blocks and the parent rock type on the shear strength of SRMs were analyzed quantitatively. Finally, some additional intrinsic behavior of SRMs was distinguished from individual experimental phenomena through the comparative analysis of many references.

2 Materials and experimental program

2.1 Material properties

The soil matrix (< 2 mm) weathered from limestone (Fig. 1a) and the rock blocks (≥ 2 mm) of slightly weathered limestone (Fig. 1b) at the same site were selected to reconstitute purified SRMs. The main properties of the soil matrix and rock blocks are shown in Tables 1 and 2, respectively. Two additional parent rock types (i.e., quartzite and granite, see Fig. 1c and d) of rock blocks were also taken into consideration to examine the influence of parent rock types. The limestone, quartzite and granite correspond to three types of rocks, i.e., sedimentary rock,

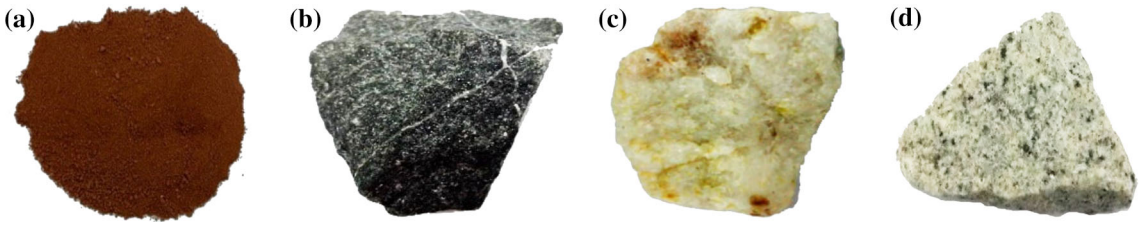

Fig. 1 Soil matrix and rock blocks used for reconstituting purified SRMs: **a** soil matrix; **b** limestone; **c** quartzite; **d** granite

Table 1 Physical properties of soil matrix

Maximum dry density (g/cm^3)	Moisture content (%)	Specific gravity	Liquid limit (%)	Plastic limit (%)
1.81	17.3	2.74	38.8	19.0

Table 2 Physical and mechanical properties of rock blocks

Parent rock	Saturated uniaxial compressive strength (MPa)	Point load strength (MPa)	Water absorption (%)	Density (g/cm^3)
Limestone	184.0	9.2	0.15	2.73
Quartzite	266.0	13.3	0.13	2.50
Granite	301.0	15.1	0.10	2.65

metamorphic rock and magmatic rock, respectively. The weathering degree of rock blocks was defined as slight weathering because they were quite fresh, intact and slightly discolored. The used rock blocks were all in angular shape and had approximated roundness.

2.2 Sample-scale structural parameters

The structure has a great influence on the mechanical behavior of SRMs [15, 16]. Because of the presence of rock blocks, the sample-scale structure is more important and meaningful to SRMs than the microscale structure. In this study, three sample-scale structural parameters (i.e., initial dry density of sample, gradation of rock blocks and spatial distribution of rock blocks) of SRMs were considered.

1. Initial dry density of sample

The initial dry density (which is termed dry density for short hereafter) of a sample evaluates how close the grains and pores are arranged in SRMs at the sample-scale. The SRM samples were prepared by compaction in five equal layers. They had three levels of dry density, i.e., 1.77 g/cm^3 (D_1), 1.89 g/cm^3 (D_2) and 2.02 g/cm^3 (D_3), which represented the loose, natural and dense states of SRMs, respectively.

2. Gradation of rock blocks

The gradation of rock blocks reflects the mean size of rock blocks and the content of each grain fraction; thus, it can indirectly characterize the sample-scale structure of SRMs. The gradation can be determined by sieve analysis. Three gradations of rock blocks in the SRMs collected from different positions of an eluvial–colluvial soil slope in Zhaoshan mountain, Hunan Province, China was taken into account [9, 12], as shown in Fig. 2. Note that among rock blocks, the grains larger than 5.0 mm are referred to as coarse grains, and the grains not larger than 5.0 mm are referred to as fine grains [25, 39].

3. Spatial distribution of rock blocks

In the natural environment, rock blocks are not homogeneously distributed in SRMs but have various spatial distributions. Three typical spatial distributions of rock blocks in the shallow SRMs strata of an alluvial piedmont fan were selected to prepare samples. In Fig. 3b, S_1, S_2 and S_3 represent the spatial distributions of rock blocks in the proximal fan, medial fan and distal fan, respectively. In the S_1 form, rock blocks are homogeneously distributed in the sample, showing the best integrity. In the S_2 form, the spatial distribution of rock blocks is inhomogeneous and the integrity of the sample is the worst. In the S_3 form, rock blocks are concentrated in the middle part of the sample, showing the intermediate integrity.

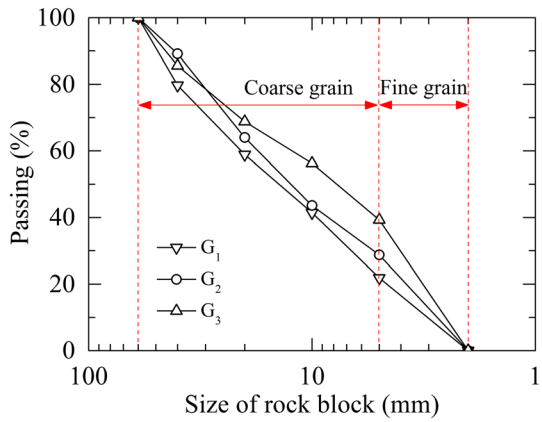

Fig. 2 Three typical gradation types of rock blocks

At a given rock block content, the more concentrated rock blocks are, the more complex the structure of the SRM sample is. With this in mind, the standard deviation was proposed to quantify the structural complexity. The standard deviation is expressed by:

$$\sigma = \sqrt{\left[\frac{1}{N}\sum_{i=1}^{N}(x_i - \mu)^2\right]} \quad (1)$$

where σ is the standard deviation; μ is the mean value; $N = 5$ is the number of soil layers; x_i is the cumulative height of rock block layers.

Table 3 shows the calculation results. In this table, E is the normalized value of σ and termed the coefficient of structural homogeneity. The larger the value of E is, the more homogeneous the spatial distribution of rock blocks is, and the simpler the structure of the SRM sample is.

2.3 Experimental program

2.3.1 Test instrument

Triaxial tests were performed in the SZ30-4D large-scale triaxial apparatus (Chengdu Donghua Zhuoyue Technology Co., Ltd, China) (Fig. 4), which is capable of applying a maximum axial stress of 17 MPa and a maximum confining pressure of 3 MPa. This apparatus can automatically acquire all test parameters such as axial stress, axial strain, confining pressure, pore water pressure, volumetric strain and displacement.

2.3.2 Triaxial tests on purified SRMs affected by structural parameters

To study the influence of structures on the mechanical behavior of SRMs, consolidated drained triaxial compression tests were carried out on SRM samples, whose rock blocks were come from a single parent rock (i.e., slightly weathered limestone). Since the rock block content of SRMs usually falls in the range of 25–75% [51], a relative small value of 30% was considered in this section. The SRM samples were 300 mm in diameter and 600 mm in height. The method for sample preparations was similar to those used by Huang et al. [18] and Zhang et al. [48]. To facilitate the comparison with the existing research results, different shear rates (i.e., 0.5 mm/min (V_1), 1.0 mm/min (V_2) and 1.5 mm/min (V_3)) and confining pressures (i.e., 200 kPa, 300 kPa and 400 kPa) were used in the tests. The triaxial tests were arranged according to the orthogonal array table L_{18} (3^4), as shown in Table 4. The room temperature remained at about 23 °C during triaxial tests.

2.3.3 Triaxial tests on purified SRMs affected by the parent rock type of rock blocks

The parent rock type is an easy-to-determine comprehensive index and is independent on weathering. Hence, it is of practical significance for engineers to evaluate the mechanical behavior of SRMs based on parent rock types. In this section, a series of consolidated drained triaxial compression tests were conducted on SRM samples, whose rock blocks were slightly weathered and come from three different parent rocks (i.e., limestone, quartzite and granite). The G_1 gradation of rock blocks, a median dry density of sample (D_2), the homogeneous spatial distribution of rock blocks (S_1), a shear rate of 1.0 mm/min (V_2) and a median rock block content of 50% were considered. The triaxial tests were repeated under different confining pressures (i.e., 200 kPa, 300 kPa and 400 kPa). The specification of triaxial tests is presented in Table 5.

2.4 Assessment of the reproducibility of test results

Two parallel triaxial tests were conducted under a confining pressure of 200 kPa following the test specification of case 1 to assess the reproducibility of the test results of purified SRMs. The results of the verification tests are

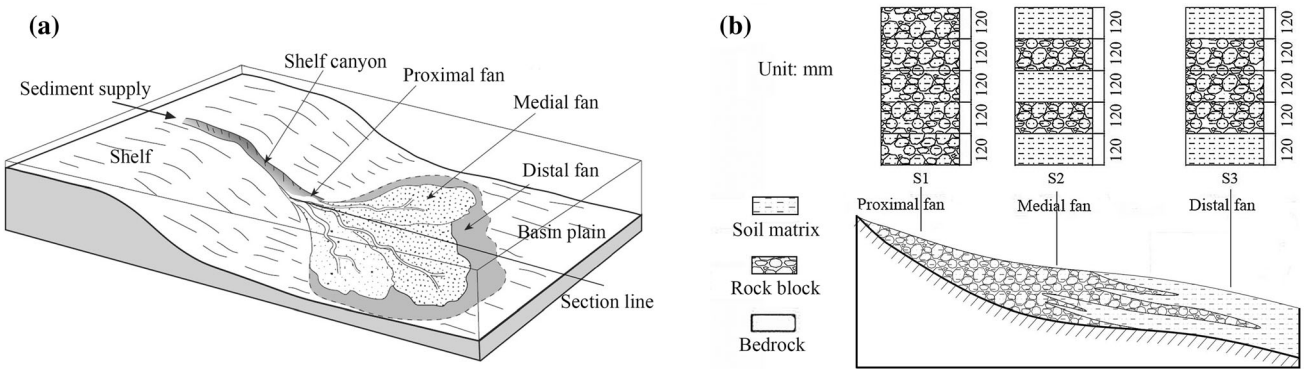

Fig. 3 Sketches of alluvial piedmont fan and gradations: **a** alluvial piedmont fan (Nichols, 2009); **b** typical spatial distributions of rock blocks

Table 3 Quantification of the structural complexity of SRM samples

Typical spatial structure	X_i	μ	σ	E
S_1	120, 240, 360, 480, 600	360	169.71	1.00
S_2	0, 120, 120, 240, 240	144	89.76	0.53
S_3	0, 120, 240, 360, 360	216	139.92	0.82

Fig. 4 The SZ30-4D large-scale triaxial apparatus

illustrated in Fig. 5. It is noted that the two stress–strain curves were in good agreement. The peak deviator stresses obtained from the two tests were 431.9 kPa and 429.5 kPa, respectively, showing good consistency. Moreover, the elastic modulus of SRMs given by the first test was 170.9 kPa, which was also very close to that (i.e., 166.7 kPa) calculated from the results of the second test. This indicates that under the same condition, good reproducibility of test data could be ensured using the purified SRM materials based on the abstraction idea.

3 Mechanical behavior of purified SRMs

The mechanical behavior of SRMs is complicated and affected by many hidden factors (e.g., structural parameters and parent rock type). In this study, the SRM samples were properly purified based on the abstraction idea, which could help reveal the intrinsic behavior of SRMs.

3.1 Inductive analysis of the test data

3.1.1 Stress–strain relationship

Figure 6 shows the stress–strain relationships and failure features of SRM samples in various cases. All the stress–strain curves could be divided into two types according to their shapes. The first type of curve was relatively smooth and occurred when the sample had the G_2 or G_3 gradation

Table 4 Cases of triaxial tests on purified SRMs affected by structural parameters

Case	Gradation of rock blocks	Dry density of sample	Spatial distribution of rock blocks	Shear rate	Parent rock	Weathering degree	Rock block content (%)
1	G_1	D_1	S_1	V_1	Limestone	Slight weathering	30
2	G_1	D_2	S_2	V_2	Limestone	Slight weathering	30
3	G_1	D_3	S_3	V_3	Limestone	Slight weathering	30
4	G_2	D_1	S_2	V_3	Limestone	Slight weathering	30
5	G_2	D_2	S_3	V_1	Limestone	Slight weathering	30
6	G_2	D_3	S_1	V_2	Limestone	Slight weathering	30
7	G_3	D_1	S_3	V_2	Limestone	Slight weathering	30
8	G_3	D_2	S_1	V_3	Limestone	Slight weathering	30
9	G_3	D_3	S_2	V_1	Limestone	Slight weathering	30

Table 5 Cases of triaxial tests on purified SRMs affected by parent rock type of rock blocks

Case	Parent rock	Weathering degree	Gradation of rock blocks	Dry density of sample	Spatial distribution of rock blocks	Shear rate	Rock block content (%)
10	Limestone	Slight weathering	G_1	D_2	S_1	V_2	50
11	Quartzite	Slight weathering	G_1	D_2	S_1	V_2	50
12	Granite	Slight weathering	G_1	D_2	S_1	V_2	50

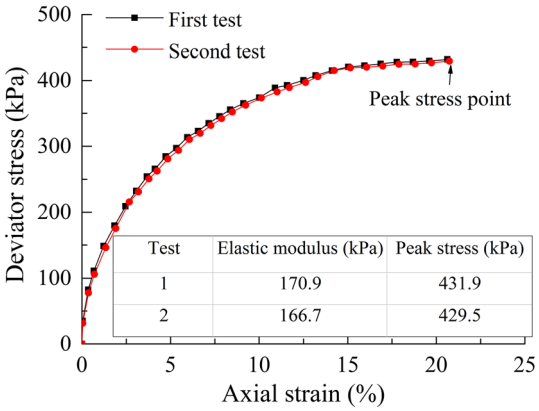

Fig. 5 Assessment of the reproducibility of triaxial test results

(i.e., cases 4–9) of rock blocks and was subjected to a low confining pressure. The second type of curve showed an obvious "step-like" feature at a large axial strain and mainly took place when the sample had the G_1 gradation (i.e., cases 1–3) of rock blocks and was subjected to a high confining pressure. This is partly because there are more coarse grains in the sample when rock blocks follow the G_1 gradation. In this case, the shear strength of the material mainly comes from the friction among rock blocks. At a large shear stress, some rock blocks may be forced to slide or crush (especially for angular ones), which leads to the fluctuation of the stress–strain curve.

To examine the influences of different factors, the results of different cases were averaged, which is a common analysis method in orthogonal tests. For instance, three average values were calculated from the data of the cases 1–3, 4–6 and 7–9 with different gradation types of rock blocks, respectively. In this manner, the influences of the dry density of sample (D), spatial distribution of rock blocks (S) and shear rate (V) were offset, and these average values could be used to study the influence of the gradation of rock blocks (G). Analyzing the test results of SRMs with a single parent rock type of rock blocks (i.e., cases 1–9), one can obtain the following findings:

- The larger the coarse grain content (e.g., cases 1–3 with G_1 gradation) was, the more likely the coarse grains contacted each other. As the positions of coarse grains adjusted, the local skeleton structure was gradually stable, and the shear stress became mainly borne by the skeleton structure formed by coarse grains. Thus, the initial stage of the stress–strain curve was steeper at a larger coarse grain content.
- The higher the dry density of sample was, the larger the contact area between rock blocks was, and the larger the friction among coarse grains. Therefore, the initial stage of the stress–strain curve was steeper as the dry density increased. When the shear stress exceeded the peak shear strength, individual angular rock blocks began to crush and the shear strength decreased, showing a strain-softening phenomenon.
- The deformation and failure feature of SRMs were significantly affected by the spatial distribution of rock blocks and shear rate. At a low rock block content (i.e., 30%), when rock blocks were distributed in the S_1 form and S_3 form, the failures of the SRM samples were characterized by two modes depending on the shear rate. At a shear rate of 0.5 mm/min, the samples showed a homogeneous deformation (Fig. 6a and e). Nevertheless, at a shear rate of 1.0 mm/min or 1.5 mm/min, the samples showed a swelled deformation (Fig. 6c, f, g and h): the middle parts of the samples swelled obviously and the swelling tended to decrease from the middle to the two ends. When rock blocks were distributed in the S_2 form, the failure mode of the samples was characterized by a layered deformation (Fig. 6b, d and i). In this case, the soil matrix layers in the middle expanded outward slightly, while the soil matrix layers near the two sample ends had no obvious deformation. By contrast, because rock blocks were penetrated into the adjacent soil matrix layers under triaxial loading, the rock block layers shrank inward.
- When the confining pressure was large, the nonlinear stress–strain curve of SRMs was in good agreement with the hyperbolic law proposed by Duncan and Chang [10]. Under the confining pressure of 200 kPa, there

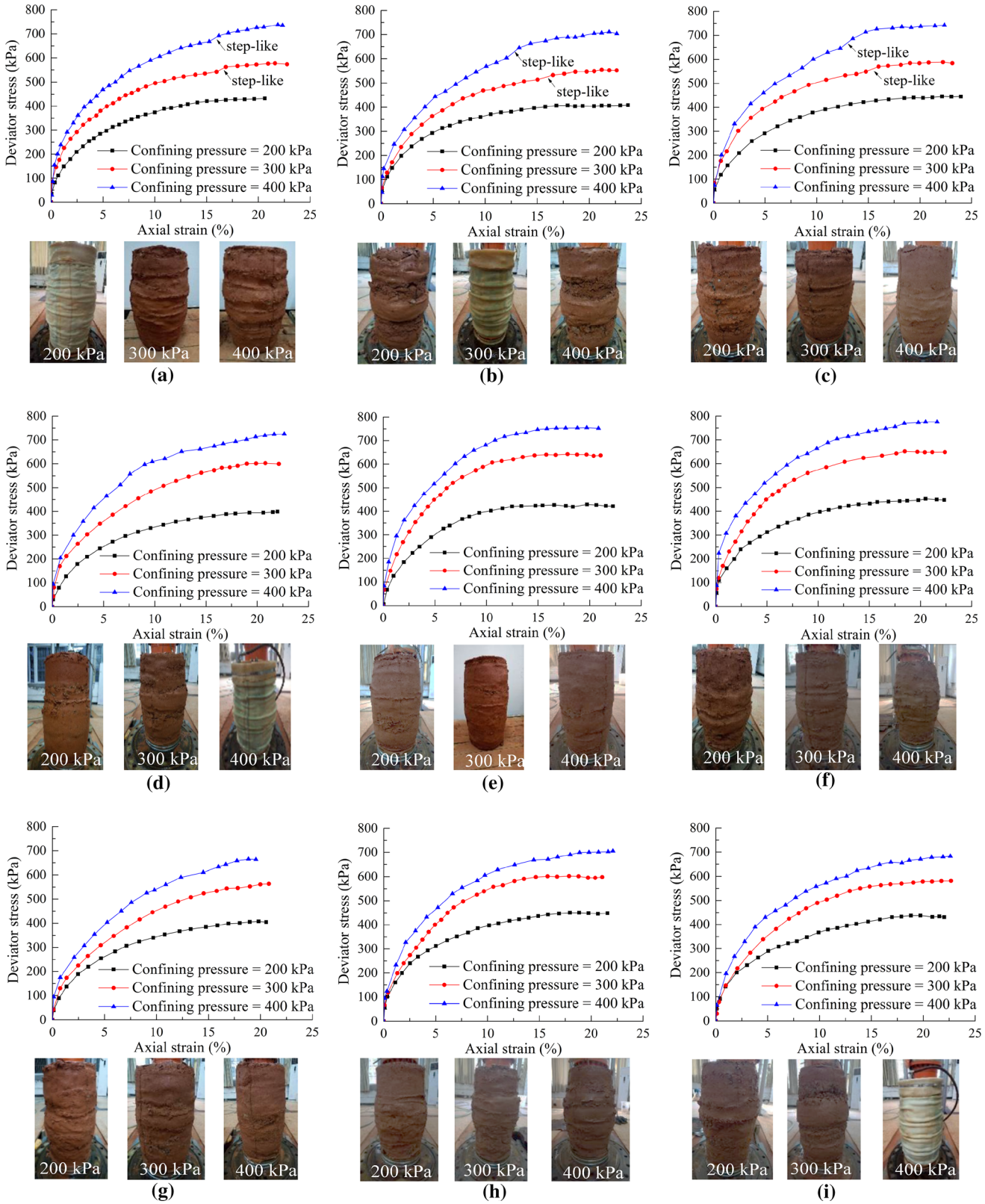

Fig. 6 Stress-strain curves and failure features of the samples in different cases: **a** case 1; **b** case 2; **c** case 3; **d** case 4; **e** case 5; **f** case 6; **g** case 7; **h** case 8; **i** case 9; **j** case 10; **k** case 11; **l** case 12

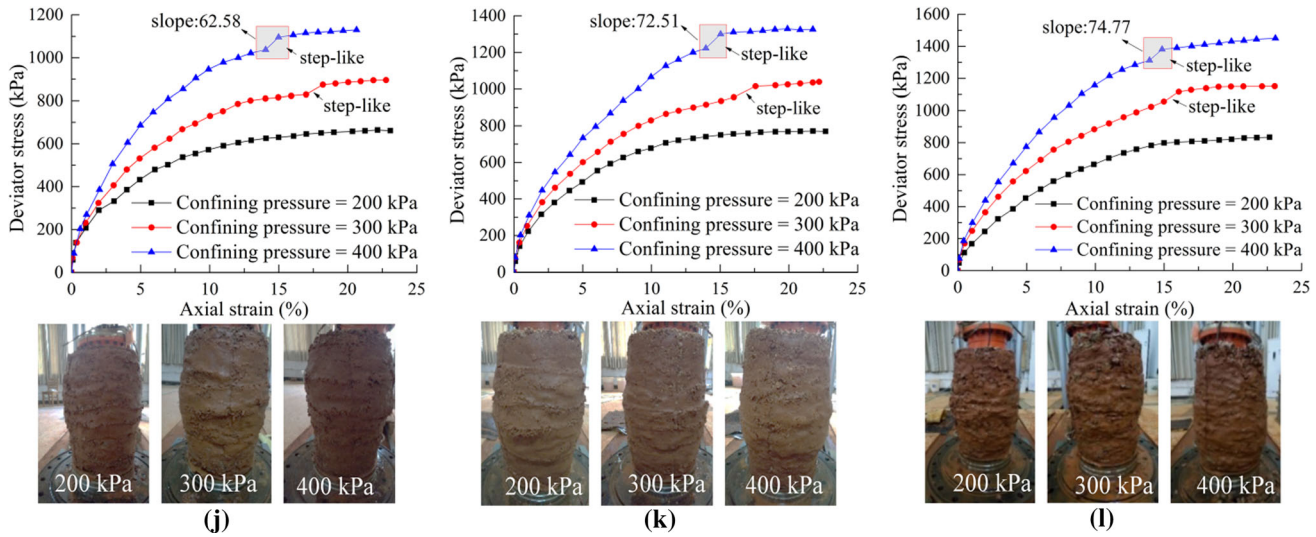

Fig. 6 continued

was no significant difference in the peak deviator stresses between the SRMs with various gradations of rock blocks. As the confining pressure increased, the peak deviator stress reached the maximum when SRMs had the G_2 gradation of rock blocks. This means that there was an optimum gradation that enabled coarse grains and fine grains to better resist shear stress together, producing the best mechanical performance of SRMs.

Figure 6j–l depicts the stress–strain relationships and failure features of the samples affected by the parent rock type of rock blocks. One can note that the peak deviator stress was increasingly larger as the parent rock type of rock blocks varied from limestone to quartzite and then to granite. This is because the surface roughness and uniaxial compressive strength of the limestone rock blocks were the smallest and those of the granite rock blocks were the largest. Furthermore, it is observed that the increment of deviator stress at the step-like point was the smallest when the parent rock type of rock blocks was limestone while that was the largest when the parent rock type of rock blocks was granite. This is likely due to the fact that a larger stress is needed for the rock blocks of a higher uniaxial compressive strength to crush.

3.1.2 Volumetric deformation

Under the drained condition, the SRM samples either dilate or contract, which is termed dilatancy. Dilatancy has a significant effect on the physical and mechanical properties, so it is necessary to analyze the volumetric deformations of SRMs. Figure 7 illustrates the relationship between the volumetric strain and axial strain of SRMs in various cases. Note that the positive volumetric strain is plotted downward. It is observed that the volumetric strains of all samples were positive before the tests were stopped, exhibiting contractive behavior. The influence of the confining pressure, gradation of rock blocks and dry density of sample on the volumetric deformation of the SRM samples are summarized as follows:

- The dilatancy characteristics of SRMs were significantly affected by confining pressures. At a relatively high confining pressure (i.e., 300 kPa or 400 kPa), the volumetric strain went on rising and the sample always contracted as the axial strain increased. As the confining pressure decreased, the initial slope of the curves and the volumetric strain were slightly reduced. However, at a low confining pressure (i.e., 200 kPa), the volumetric strain first increased and then decreased with increasing axial strain, showing a dilative tendency in the end. This is because at a low confining pressure, the sample was first compressed due to the position adjustment of soil grains with the increase in axial strain. As the axial strain reached a certain high value, the low lateral pressure allowed the climbing of soil grains over one another, and thus, the sample tended to dilate. By contrast, soil grains were not easy to climb over one another at a high confining pressure due to a large lateral pressure, but the grain breakage phenomenon might occur instead. The crushed grains filled the pores and further restrained the movement of grains, so the sample always showed contractive behavior at a high confining pressure.
- When the gradation of rock blocks was G_1 (which corresponded to the highest coarse grain content), the volumetric strain was generally the largest, and the

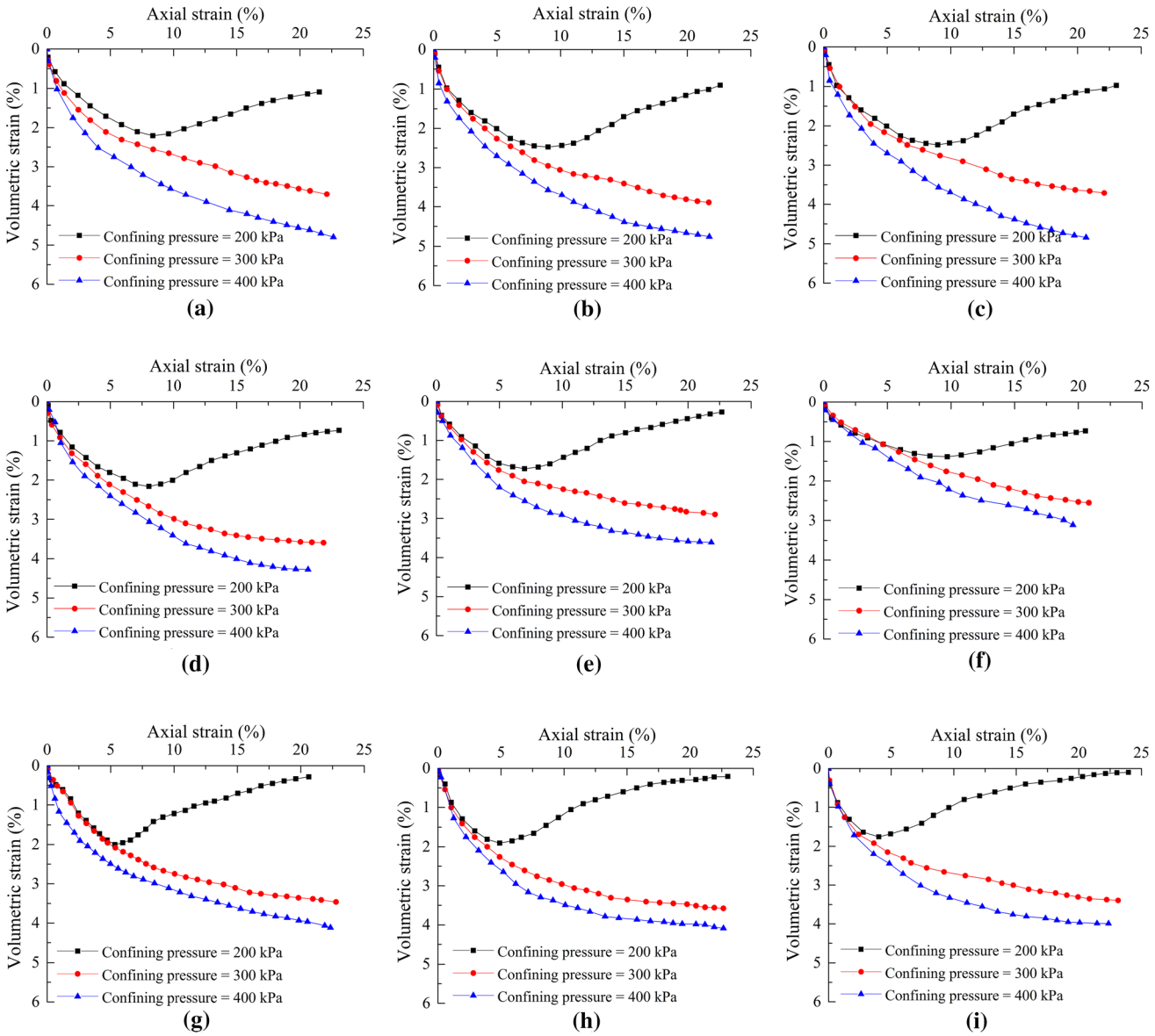

Fig. 7 Volumetric strain–axial strain curves of the samples in different cases: **a** case 1; **b** case 2; **c** case 3; **d** case 4; **e** case 5; **f** case 6; **g** case 7; **h** case 8; **i** case 9

volumetric strain decreased with the increase in the dry density of sample. This is expected since soil grains of various sizes were easy to adjust and fill the gaps among them under triaxial loading when the sample was loose.

- At a confining pressure of 200 kPa, the dilative tendency of the SRM samples became increasingly significant with the increase in the dry density of sample. Moreover, as the confining pressure increased, no matter how large the dry density was, the sample was always in shear contraction. This suggests that the volumetric deformations of SRMs were not only affected by the initial compaction state but also influenced by the stress state.

3.1.3 Shear strength parameters

Table 6, 7, and 8 summarizes the shear strength parameters (i.e., cohesion and angle of internal friction) of the SRM samples affected by three structural parameters and shear rate (i.e., cases 1-9). It is noted that when the coarse grain content decreased (e.g., the gradation of rock blocks varied from G_1 to G_3), the cohesion first decreased slightly and then increased substantially, and the angle of internal friction first increased and then reduced considerably. Meanwhile, as the dry density of sample increased, the cohesion increased greatly while the angle of internal friction did not change significantly. These results indicate that the grain size and porosity have visible influences on

the shear strength parameters of SRMs. A further analysis about this will be conducted in Sect. 4. In addition, the spatial distribution of rock blocks has a great influence on the cohesion but has little influence on the angle of internal friction. Generally, the more homogeneous the spatial distribution of rock blocks was (e.g., in the S_1 form with E = 1.00), the larger the cohesion of SRMs was. This is because if rock blocks are homogeneously distributed, they can be well bonded by soil matrix.

The significance of three structural parameters (i.e., dry density of sample, gradation of rock blocks, spatial distribution of rock blocks) and shear rate affecting the cohesion and angle of internal friction were evaluated by range analyses, and the results are shown in Tables 7 and 8. One can note that according to the significance of their influences on the shear strength parameters, the examined factors can be arranged in the following order: the gradation of rock blocks, the dry density of sample, the spatial distribution of rock blocks and the shear rate.

Table 9 and Fig. 8 present the influence of the parent rock type of rock blocks on the shear strength parameters of the purified SRMs. The parent rock type was represented by the saturated uniaxial compressive strength. It is noted that the influence of the parent rock type of rock blocks on the cohesion was not significant since the cohesion of SRMs mainly came from the soil matrix. By contrast, the angle of internal friction increased almost linearly with the increase in the saturated uniaxial compressive strength of rock blocks. This is mainly because the rock blocks with different parent rock types had different surface roughness, and thus, there were different friction coefficients among rock blocks in the loading process. Among the three types of parent rock, granite had the largest surface roughness, so the angle of internal friction of the SRM sample made of granite rock blocks was the largest.

3.1.4 Initial elastic modulus

The elastic modulus is also an important mechanical property of SRMs. According to Duncan and Chang [10], the relationship between the deviator stress and axial strain can be expressed by the following equation:

$$\frac{\varepsilon_a}{\sigma_1 - \sigma_3} = a + b\varepsilon_a \tag{2}$$

where ε_a is the axial strain; σ_1-σ_3 is the deviator stress; a and b are two constants.

Then, the initial elastic modulus can be calculated by:

$$E_i = \frac{1}{a} \tag{3}$$

where E_i is the initial elastic modulus.

In this way, the initial elastic moduli of the purified SRMs with a single parent rock type of rock blocks (i.e., cases 1–9) were calculated, as shown in Table 10. It is noted that as the increase in the confining pressure, the initial elastic modulus always increased, but its increment was not the same due to the influence of different structural parameters.

At a low confining pressure, the initial elastic modulus did not differ much when the gradation of rock blocks varied. But at high confining pressure, the initial elastic modulus obviously increased with increasing coarse grain content. As the increase in the dry density of sample, the pores in the sample decreased and the sample became stiff, so the initial elastic modulus increased significantly. When rock blocks were distributed homogeneously (i.e., in the S_1 form with E = 1.00), the soil matrix could fill the gaps among rock blocks well and the sample was of good integrity, leading to a relatively large initial elastic modulus. By contrast, when the spatial distribution of rock blocks was inhomogeneous (i.e., in the S_2 form with E = 0.53), the integrity of the sample was worse and rock

Table 6 Shear strength parameters of SRMs affected by structural parameters

Case	Gradation of rock blocks	Dry density of sample	Spatial distribution of rock blocks	Shear rate	Cohesion c (kPa)	Angle of internal friction φ (°)
1	G_1	D_1	S_1	V_1	38.9	25.66
2	G_1	D_2	S_2	V_2	32.8	25.53
3	G_1	D_3	S_3	V_3	46.4	25.21
4	G_2	D_1	S_2	V_3	25.1	26.81
5	G_2	D_2	S_3	V_1	34.5	26.94
6	G_2	D_3	S_1	V_2	42.4	26.68
7	G_3	D_1	S_3	V_2	51.8	23.14
8	G_3	D_2	S_1	V_3	68.0	22.89
9	G_3	D_3	S_2	V_1	66.0	22.40

Table 7 Range analysis of cohesion (Unit: kPa)

Factor	Gradation of rock blocks	Dry density of samples	Spatial distribution of rock blocks	Shear rate
Mean value I	39.4	38.6	49.8	46.5
Mean value II	34.0	45.1	41.3	42.3
Mean value III	61.9	51.6	44.2	46.5
Range *R*	27.9	13.0	8.5	4.2

Table 8 Range analysis of the angle of internal friction (Unit: °)

Factor	Gradation of rock blocks	Dry density of samples	Spatial distribution of rock blocks	Shear rate
Mean value I	25.47	24.76	25.08	25.00
Mean value II	26.81	25.12	24.91	25.12
Mean value III	22.81	25.20	25.10	24.97
Range *R*	4.00	0.44	0.18	0.15

Table 9 Shear strength parameters of SRMs affected by parent rock type of rock blocks

Case	Parent rock	Saturated uniaxial compressive strength (MPa)	Cohesion *c* (kPa)	Angle of internal friction φ (°)
10	Limestone	184.0	54.20	32.55
11	Quartzite	266.0	55.00	35.52
12	Granite	301.0	54.40	37.37

blocks could easily penetrate into soil matrix layers, giving rise to the decrease in the initial elastic modulus.

3.2 Quantitative relationship between hidden factors and shear strength

3.2.1 Relationship between the parent rock type and shear strength

The shear strengths of the purified SRMs with different parent rock types of rock blocks were fitted with a 3D surface, as shown in Fig. 9. It is noted that for the SRMs of a given parent rock type of rock blocks, the shear strength increased linearly with increasing confining pressure. Meanwhile, under a given confining pressure, the greater the saturated uniaxial compressive strength of rock blocks was, the higher the shear strength of SRMs was.

The relationship among the shear strength (τ), saturated uniaxial compressive strength (R_c) and confining pressure (σ_3) can be expressed by the following equation ($R^2 = 0.99$):

$$\tau = \frac{A_1 + A_2 R_c + A_3 R_c^2 + A_4 \sigma_3}{1 + A_5 R_c} \quad (4)$$

where $A_1 = 264$, $A_2 = -0.926$, $A_3 = -0.0012$, $A_4 = 1.695$ and $A_5 = -0.0016$ are fitting parameters.

Therefore, if the confining pressure is constant and the structural parameters remain the same, the shear strengths of the SRM samples with different parent rock types of

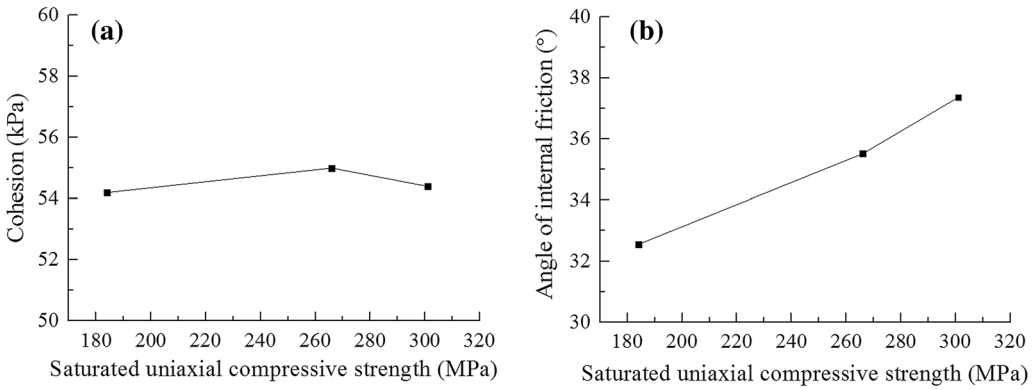

Fig. 8 Relationship between the parent rock type of rock blocks and shear strength parameters: **a** cohesion; **b** angle of internal friction

Table 10 Average initial elastic moduli of SRMs under different confining pressures (Unit: kPa)

Confining pressure	Gradation of rock blocks			Dry density of sample			Spatial distribution of rock blocks		
	G_1	G_2	G_3	D_1	D_2	D_3	S_1	S_2	S_3
200	186	181	176	149	209	215	199	170	174
300	259	240	199	207	251	259	252	203	243
400	290	278	243	248	293	300	313	248	280

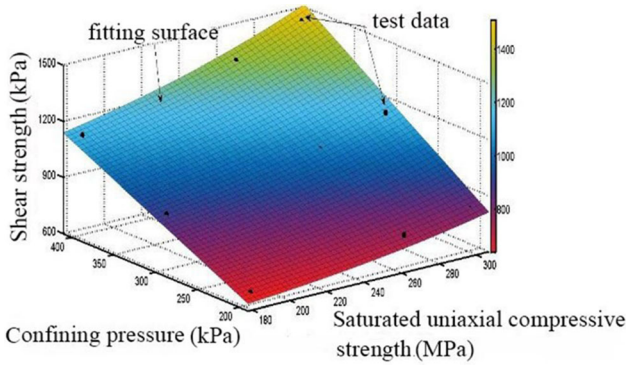

Fig. 9 Shear strength of SRMs affected by the parent rock type of rock blocks

rock blocks can be calculated from the R_c values of rock blocks without testing.

3.2.2 Relationship between the spatial distribution of rock blocks and shear strength

A 3D surface is also obtained by fitting the data of the shear strength (τ), coefficient of structural homogeneity (E) and confining pressure (σ_3), as shown in Fig. 10. The coefficient of structural homogeneity quantifies the spatial distribution of rock blocks. This 3D surface has the following expression ($R^2 = 0.98$):

$$\tau = B_1 + B_2(\ln E)^2 + B_3\sigma_3 \quad (5)$$

where $B_1 = 152.4$, $B_2 = -92.08$ and $B_3 = 1.465$ are fitting parameters.

According to Eq. (5) and Fig. 10, for the SRMs of a given parent rock type of rock blocks, the shear strength increased linearly with increasing confining pressure. Furthermore, under a given confining pressure, the higher the coefficient of structural homogeneity was, the greater the shear strength of SRMs was. This indicates that the spatial distribution of rock blocks had a considerable influence on

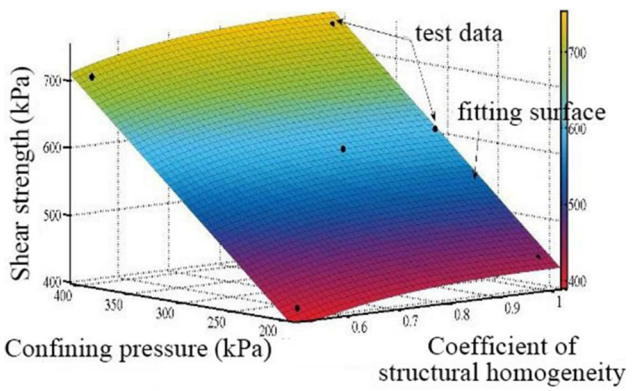

Fig. 10 Shear strengths of SRMs affected by the spatial distribution of rock blocks

the mechanical behavior of SRMs. Therefore, much attention should be paid to the distribution characteristics of rock blocks when addressing the mechanical problems with SRMs.

4 Discussion on the mechanical behavior of SRMs

To extract the intrinsic behavior of SRMs and provide reliable guidance for engineering practice, many representative references were selected for comparative analysis. The test methods used in these references were all large-scale triaxial tests. Because the materials were reasonably purified, the test results of this study were convenient to be compared with those reported in the literature.

4.1 Effect of dry density

In this section, the effect of dry density on the shear strength parameters of SRMs was discussed based on the results obtained in this study and those reported in the literature [3, 19, 29, 30].

Figure 11 presents some typical stress–strain curves of the SRM samples with different levels of dry density. When the dry density is large, the soil matrix fills well the gaps among rock blocks. Once the shear stress exceeds the shear strength under a small confining pressure, the structure of the material varies and becomes loose. Thus, the stress–strain curve shows a strain-softening trend, which is consistent with the test results presented in Sect. 3.1.1. Nevertheless, when the confining pressure is high, the increase in the shear stress leads some rock blocks to crush, then the broken grains fill the pores and the material becomes denser. As a result, the material shows strain-hardening behavior no matter how large or small the dry density is. This means that the strain-softening behavior of SRMs is related to both the dry density and confining pressure.

Figure 12 shows the relationships between the dry density and shear strength parameters (i.e., cohesion and angle of internal friction) of SRMs. One can note some differences among the results of different previous studies. However, based on the principle of "seeking common ground while reserving differences," some general findings can be summarized from Fig. 12. In most cases, both the cohesion and angle of internal friction show a more or less linear increase as the dry density increases. This variation of cohesion with dry density appears reasonable because the increase in dry density enhances the bonding among soil matrix and rock blocks. The effect of dry density on the angle of internal friction is closely related to the interlocking forces and friction among rock blocks. As the

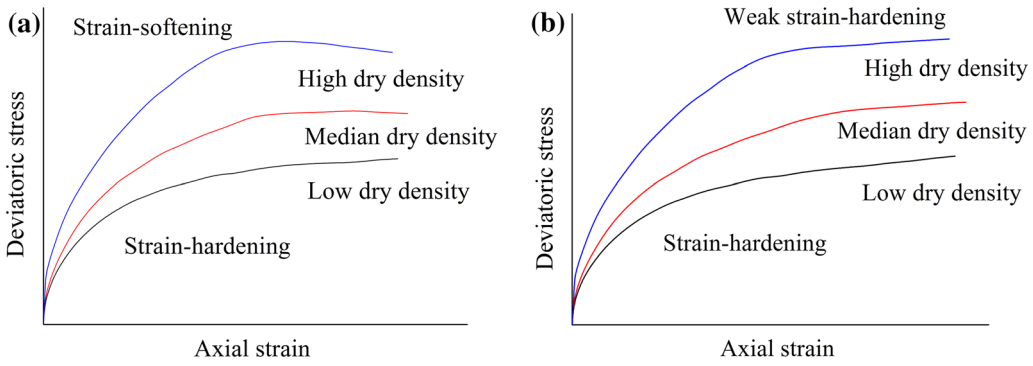

Fig. 11 Typical stress–strain curves of SRMs affected by dry density: **a** low confining pressure; **b** high confining pressure

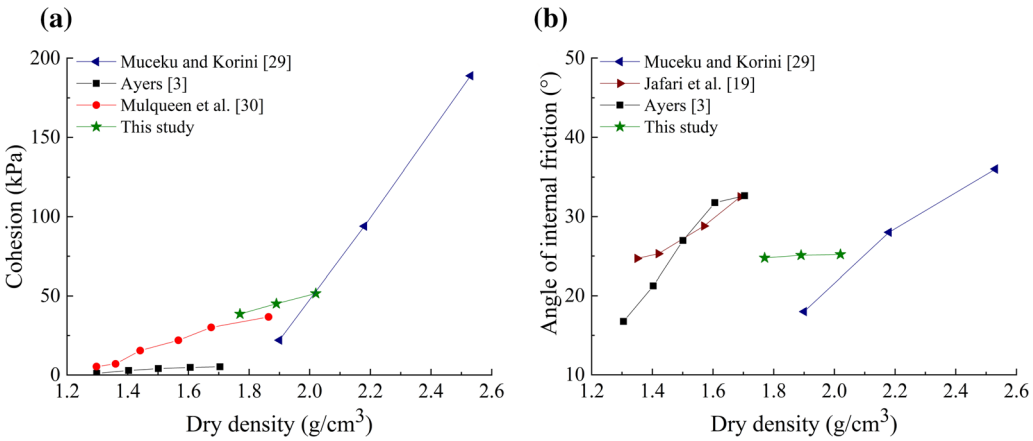

Fig. 12 Relationships between dry density and shear strength parameters: **a** cohesion; **b** angle of internal friction

dry density increases, the interlocking and friction among rock blocks are enhanced under triaxial loading, causing the rise in the angle of internal friction.

4.2 Effect of gradation

Many previous studies such as Seif El Dine et al. [34], Afifipour and Moarefvand [1], Khorasani et al. [22], Wang et al. [42], and Zhang et al. [48] among others found that the gradation had an obvious influence on the mechanical properties of SRMs. Some studies (Tang et al. [39]; Vallejo [41]; Hu et al., [17]; Chen et al., [7]; Yang et al., [47]) also reported that SRMs with the largest coefficients of uniformity usually had the highest shear strengths. The above findings are consistent with the results obtained in this work (Tables 10 and 11). However, the influence of individual grain fractions on mechanical behavior has seldom been examined. From the research of purified SRMs, it is noted that when the gradation of rock blocks was G_2, the angle of internal friction was the maximum, the cohesion achieved the minimum and the shear strength was the maximum (Tables 7, 8 and 11). For the samples with the G_2 gradation, the content of each grain fraction fell between those of the grain fractions in the samples with the G_1 and G_3 gradations except for the coarse grain fraction of 40–60 mm (see Fig. 2); nevertheless, they had the largest shear strength rather than the intermediate (Table 11). This means that the influence of gradation on the shear strength parameters of SRMs is mainly controlled by the content of the grains between 40 mm and 60 mm. Therefore, the study of gradation should be refined to the contents of specific grain fractions.

The effect of gradation on the mechanical properties of SRMs is closely related to the porosity. When SRMs are well graded, fine grains and soil matrix fill the voids among coarse grains (i.e., reduces the porosity), so the shear strength and elastic modulus of SRMs are enhanced.

4.3 Effect of rock block content

To examine the effect of rock block content on the mechanical behavior of SRMs, the results reported by Cen et al. [4], Coli et al. [8], Huang et al. [18], Seif El Dine et al. [34], Wang et al. [42], Napoli et al. [31] and Sonmez et al. [38] were compared.

Table 11 Effect of rock block gradation on the shear strength of SRMs

Gradation of rock blocks	Coefficient of uniformity of rock blocks	Content of grains between 40 and 60 mm (%)	Mean shear strength of SRMs (kPa)
G_1	9.2	20.3	577.2
G_2	10.4	10.9	592.2
G_3	10.2	14.4	565.9

Figure 13 illustrates the relationships between the rock block content and shear strength parameters (i.e., cohesion and angle of internal friction). It shows that the results vary between different references. However, one can note that the cohesion generally shows a decreasing trend as the rock block content increases. When the rock block content increases from 60 to 80%, the decrease in cohesion is the most significant. A few results differed from the above general behavior of SRMs, such as the relationship between the rock block content and cohesion reported by Huang et al. [18]. This confirms the idea that special attention should be paid to properly distinguish the intrinsic behavior from individual experimental phenomena when studying the mechanical behavior of SRMs.

4.4 Further discussion

There were noticeable differences in the results of the references mentioned in Figs. 12 and 13, which may be attributed to the influences of some hidden factors of SRMs (e.g., weathering degree, parent rock type and structure).

4.4.1 Effect of weathering difference

Weathering damages the rock integrity, causes an increase in the porosity of rocks and reduces the uniaxial compressive strength of rocks (Tuğrul [40]). Therefore, the weathering degree can be characterized by the saturated uniaxial compressive strength of rock blocks. As shown in Fig. 9, the saturated uniaxial compressive strength of rock blocks had a great influence on the mechanical behavior of SRMs. This suggests that the mechanical behavior of SRMs is also highly affected by the weathering degree. Moreover, as a hidden factor, the weathering degree interferes with the study of the influence of structural parameters on the mechanical behavior of SRMs. For example, Zhang et al. [50] observed an abnormal increase in the cohesion at a rock block content of 35–60%, which could attribute to the use of strongly weathered rocks. And Wei et al. [44] also observed an increase in the macro-cohesion strength of the SRM sample, which was believed to be caused by the breakage of strongly weathered rock blocks in the shearing process. It indicates that the results may be different if the samples were made from the rock blocks with different weathering degrees. In this study, the weathering degree of all rock blocks was slight weathering, so the interference of weathering difference on the test results could be eliminated.

4.4.2 Effect of parent rock differences

Comparing and analyzing the test results of the SRMs with different parent rock types of rock blocks (see Fig. 6, cases 10–12), one can note that the parent rock differences had a significant influence on the shear strength of SRMs. Specifically, the shear strength of SRMs showed an approximately linear increase as the parent rock of rock blocks varied from limestone to quartzite and then to granite (Fig. 9). This finding was in agreement with the results of some existing references [2, 5]. The shear strength of SRMs generally comes from the comprehensive effect of the parent rock strength, the bonding among soil matrix and rock blocks, and the friction and interlocking forces among rock blocks. When the shape and surface

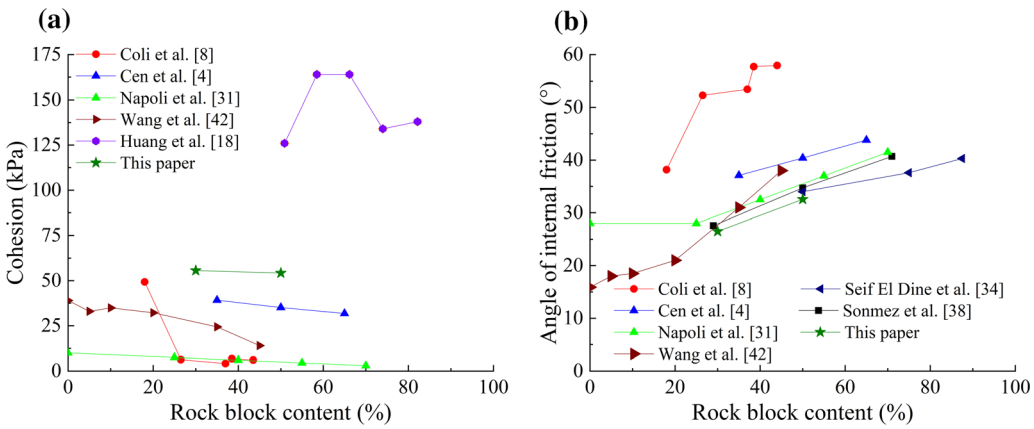

Fig. 13 Relationships between rock block content and shear strength parameters: **a** cohesion; **b** angle of internal friction

roughness of rock blocks are identical, the difference in the shear strengths of SRMs may be mainly attributed to the influence of the parent rock strength. On the other hand, the parent rock type shows little influence on the deformation characteristics of SRMs while has a certain effect on the shear strength of SRMs. It is found that at a given rock block content, the angle of internal friction decreased and the cohesion varied little with the reduction in the saturated uniaxial compressive strength of rock blocks (see Table 9). This is because the rock blocks with a smaller uniaxial compressive strength are more likely to soften and crush under saturated loading conditions, which results in a decrease in the surface roughness of rock blocks and the angle of internal friction of SRMs.

It should be noted that the influence of parent rock type on mechanical properties of SRMs may be not as significant as those of some specific parameters (e.g., particle shape, contact friction and particle crushing characteristics). However, because the parent rock type is easy to determine in engineering practice, it is a feasible and efficient index for the preliminary judgment of the mechanical properties of SRMs.

4.4.3 Effect of structural differences

In different engineering practices, SRMs may have different structural features and are often not homogeneous. As presented in Sect. 3, the spatial distribution of rock blocks had considerable effects on the shear strength parameters and elastic moduli of SRMs. When rock blocks are homogeneously distributed in the SRM sample, the sample has good integrity and a high shear strength. By contrast, when the distribution of rock blocks is inhomogeneous, stress concentrations easily occur in the SRM sample, which reduces the shear strength of SRMs. On the other hand, the spatial distribution of rock blocks also affects the deformation of SRMs [46]. When rock blocks are distributed in the S_1 or S_3 form, the shear surface initiated in the middle part is easy to propagate toward the two ends of the sample, so the sample shows a homogeneous deformation (at a low shear rate) or a swelled deformation (at a high shear rate). When rock blocks are distributed in the S_2 form, the middle soil matrix layer is between two dense rock block layers. In this case, the shear plane is difficult to develop toward the two ends of the sample. As a result, the two ends of the sample slightly contract while the middle part expands outward under a shear stress, and the sample shows a layered deformation. Hence, it is important to have a full understanding of the spatial distribution of rock blocks and restore the actual structure of SRMs as much as possible during mechanical tests.

5 Conclusions

The general mechanical behavior of SRMs was revealed by large-scale triaxial tests based on the abstraction idea. The influences of some hidden factors (i.e., structural parameters and parent rock type) on the mechanical behavior of SRMs were analyzed qualitatively and quantitatively. In addition, a comparative analysis of the results reported in the literature and those obtained in this study was conducted. The following conclusions can be drawn:

1. The influence of the parent rock type of rock blocks on the shear strength of SRMs could be characterized by Eq. (4). The increase in the uniaxial compressive strength of the parent rock of rock blocks led to an almost linear increase in the angle of internal friction of SRMs. Nevertheless, the change in cohesion was not obvious as the uniaxial compressive strength of the parent rock of rock blocks increased.
2. According to the significance of their influences on the mechanical behavior of SRMs, the structural parameters and shear rate are ordered as follows: the gradation of rock blocks, the dry density of sample, the spatial distribution of rock blocks, and the shear rate. The coarse grain content and confining pressure enhanced the effect of dry density on the mechanical behavior of SRMs. And the content of grains between 40 and 60 mm played a primary role in the influence of gradation on the shear strength parameters of SRMs. At a high-coarse grain content, the stress–strain curve tended to show a "step-like" feature. The higher the dry density of sample was, the more obvious the strain-softening behavior was. An increase in the dry density of sample, coarse grain content or coefficient of structural homogeneity enhanced the initial elastic modulus of SRMs.
3. At a low rock block content (i.e., 30%), the SRM samples with different spatial distributions of rock blocks showed three failure modes, i.e., homogeneous deformation, layered deformation and swelled deformation, depending on the shear rate. When rock blocks were homogeneously distributed, both the cohesion and the shear strength were the largest. When rock blocks were concentrated near the shear zone, the angle of internal friction was large. The relationship between the coefficient of structural homogeneity and shear strength was expressed by Eq. (5).
4. The weathering degree of parent rocks highly affects the test result when studying the influence of structural parameters on the mechanical behavior of SRMs.

The results presented in this work offer new insight regarding the general mechanical behavior of SRMs, which can provide reliable guidance for relevant

engineering practice. However, it should be noted that the shear strength equations (Eqs. 4 and 5) were fitted formulas based on a limited dataset, future work could be done to refine these expressions. In addition, further work could also focus on examining the influences of weathering degree and soil matrix type on the mechanical behavior of SRMs, and identifying the relationships between the shear strength and some specific factors (e.g., material composition, internal structure, friction coefficient, particle shape, contact friction and particle crushing characteristics).

6 Acknowledgements

The authors would like to acknowledge the financial support from the National Natural Science Foundation of China (No. 51108397); the Natural Science Foundation of Hunan Province, China (No. 2015JJ2136); the Key Project of Hunan Provincial Education Department, China (No. 19A477); the Hunan Key Laboratory of Geomechanics and Engineering Safety, China (No. 16GES04); and the High-level Talent Gathering Project in Hunan Province, China (No. 2019RS1059).

References

1. Afifipour M, Moarefvand P (2014) Mechanical behavior of bimrocks having high rock block proportion. Int J Rock Mech Min Sci 65:40–48
2. Alonso EE, Romero EE, Ortega E (2016) Yielding of rockfill in relative humidity-controlled triaxial experiments. Acta Geotech 11(3):455–477
3. Ayers PD (1987) Moisture and density effects on soil shear strength parameters for coarse grained soils. Trans Asae 30(5):1282–1287
4. Cen D, Huang D, Ren F (2017) Shear deformation and strength of the interphase between the soil–rock mixture and the benched bedrock slope surface. Acta Geotech 12(2):391–413
5. Charles JA, Watts KS (1980) The influence of confining pressure on the shear strength of compacted rockfill. Geotechnique 30(4):353–367
6. Chen AJ, Zhang JS (2019) Strength and deformation characteristics of silty sand improved by gravel. KSCE J Civ Eng 23(2):525–533
7. Chen XB, Li ZY, Zhang JS (2014) Effect of granite gravel content on improved granular mixtures as railway subgrade fillings. J Cent South Univ 21(8):3361–3369
8. Coli N, Berry P, Boldini D (2011) In situ non-conventional shear tests for the mechanical characterisation of a bimrock. Int J Rock Mech Min Sci 48(1):95–102
9. Dong H, Huang R, Gao QF (2017) Rainfall infiltration performance and its relation to mesoscopic structural properties of a gravelly soil slope. Eng Geol 230:1–10
10. Duncan JM, Chang CY (1970) Nonlinear analysis of stress and strain in soils. J Soil Mech Found Div 96(5):1629–1653
11. De Frias Lopez R, Silfwerbrand J, Jelagin D, Birgisson B (2016) Force transmission and soil fabric of binary granular mixtures. Géotechnique 66(7):578–583
12. Gao QF, Dong H, Huang R, Li ZF (2019) Structural characteristics and hydraulic conductivity of an eluvial-colluvial gravelly soil. B Eng Geol Environ 78(7):5011–5028
13. Gao WW, Gao W, Hu RL, Xu PF, Xia JG (2018) Microtremor survey and stability analysis of a soil-rock mixture landslide: a case study in Baidian town, China. Landslides 15(10):1951–1961
14. Gong J, Nie Z, Zhu Y, Liang Z, Wang X (2019) Exploring the effects of particle shape and content of fines on the shear behavior of sand-fines mixtures via the DEM. Comput Geotech 106:161–176
15. Gao QF, Jrad M, Hattab M, Fleureau JM, Ighil Ameur L (2020) Pore morphology, porosity and pore size distribution in kaolinitic remoulded clays under triaxial loading. Int J Geomech 20(6):04020057
16. Gao QF, Hattab M, Jrad M, Fleureau JM, Hicher PY (2020) Microstructural organization of remoulded clays in relation with dilatancy/contractancy phenomena. Acta Geotech 15(1):223–243
17. Hu MJ, Pan HL, Wei HZ, Wang R, Ying A (2013) Landslides & debris flows formation from gravelly soil surface erosion and particle losses in Jiangjia Ravine. J Mt Sci 10(6):987–995
18. Huang S, Ding X, Zhang Y (2015) Triaxial test and mechanical analysis of rock-soil aggregate sampled from natural sliding mass. Adv Mater Sci Eng 2015:1–14
19. Jafari MK, Shafiee A (2004) Mechanical behavior of compacted composite clays. Can Geotech J 41(6):1152–1167
20. Jehring MM, Bareither CA (2016) Tailings composition effects on shear strength behavior of co-mixed mine waste rock and tailings. Acta Geotech 11(5):1147–1166
21. Kalender A, Sonmez H, Medley E, Tunusluoglu C, Kasapoglu KE (2014) An approach to predicting the overall strengths of unwelded bimrocks and bimsoils. Eng Geol 183:65–79
22. Khorasani E, Amini M, Hossaini MF, Medley E (2019) Statistical analysis of bimslope stability using physical and numerical models. Eng Geol 254:13–24
23. Li CS, Zhang D, Du SS, Shi B (2016) Computed tomography based numerical simulation for triaxial test of soil-rock mixture. Comput Geotech 73:179–188
24. Lindquist ES, Goodman RE (1994) Strength and deformation properties of a physical model melange. In: Nelson PP, Laubach SE (eds) Proceedings of the 1st North American rock mechanics symposium. Balkema, Rotterdam, pp 843–850
25. Liu F, Mao X, Fan Y, Wu L, Liu WV (2020) Effects of initial particle gradation and rock content on crushing behaviors of weathered phyllite fills–A case of eastern Ankang section of Shiyan-Tianshui highway China. J Rock Mech Geotech Eng 12(2):269–278
26. Medley EW (1999) Systematic characterization of melange bimrocks and other chaotic soil/rock mixtures. Felsbau 17(3):152–162
27. Meng QX, Wang HL, Xu WY, Cai M (2018) A numerical homogenization study of the elastic property of a soil-rock mixture using random mesostructure generation. Comput Geotech 98:48–57
28. Miller EA, Sowers GF (1958) The strength characteristics of soil-aggregate mixtures & discussion. Highw Res Board Bull 183:16–23
29. Muceku Y, Korini O (2014) Landslide and slope stability evaluation in the historical town of Kruja Albania. Nat Hazard Earth Syst Sci 14(3):545–556
30. Mulqueen J, Stafford JV, Tanner DW (1977) Evaluation of penetrometers for measuring soil strength. J Terramech 14(3):137–151

31. Napoli ML, Barbero M, Ravera E, Scavia C (2018) A stochastic approach to slope stability analysis in bimrocks. Int J Rock Mech Min Sci 101:41–49
32. Niu F, Zheng H, Li A (2018) The study of frost heave mechanism of high-speed railway foundation by field-monitored data and indoor verification experiment. Acta Geotech. https://doi.org/10.1007/s11440-018-0740-8
33. Panthee S, Singh PK, Kainthola A, Das R, Singh TN (2018) Comparative study of the deformation modulus of rock mass. B Eng Geol Environ 77:751–760
34. Seif El Dine B, Dupla JC, Frank R, Canou J, Kazan Y (2010) Mechanical characterization of matrix coarse-grained soils with a large-sized triaxial device. Can Geotech J 47(4):425–438
35. Shen Z (2004) Science advocates simplicity-some remarks about adopting and adapting methods in geotechnical engineering. Chin J Geotech Eng 2004(2):299–300 **(in Chinese)**
36. Shi C, Wang SN, Liu L, Meng QX, Zhang Q (2013) Mesomechanical simulation of direct shear test on outwash deposits with granular discrete element method. J Cent South Univ 20(4):1094–1102
37. Singh TN, Kainthola A, Venkatesh A (2012) Correlation between point load index and uniaxial compressive strength for different rock types. Rock Mech Rock Eng 45(2):259–264
38. Sonmez H, Kasapoglu KE, Coskun A, Tunusluoglu C, Medley EW, Zimmerman RW (2009) A conceptual empirical approach for the overall strength of unwelded bimrocks. In: ISRM Regional Symposium, Rock Engineering in Difficult Ground Condition, Soft Rock and Karst, Dubrovnik, Croatia, pp 357–360
39. Tang Z, Dong X, Chai B, Yang Y (2014) Evaluation of particle size distribution of coal gangue through fractal method in Dongkuang mine, Heshan, China. J Mater Civil Eng 26(8):06014018
40. Tuğrul A (2004) The effect of weathering on pore geometry and compressive strength of selected rock types from Turkey. Eng Geol 75(3–4):215–227
41. Vallejo LE (2001) Interpretation of the limits in shear strength in binary granular mixtures. Can Geotech J 38(5):1097–1104
42. Wang HL, Cui YJ, Lamas-Lopez F, Calon N, Saussine G, Dupla JC, Canou J, Aimedieu P, Chen RP (2018) Investigation on the mechanical behavior of track-bed materials at various contents of coarse grains. Constr Build Mater 164:228–237
43. Wen R, Tan C, Wu Y, Wang C (2018) Grain size effect on the mechanical behavior of cohesionless coarse-grained soils with the discrete element method. Adv Civ Eng. https://doi.org/10.1155/2018/4608930
44. Wei HZ, Xu WJ, Xu XF, Meng QS, Wei CF (2018) Mechanical properties of strongly weathered rock-soil mixtures with different rock block contents. Int J Geomech 18(5):04018026
45. Xu W, Xu Q, Hu R (2011) Study on the shear strength of soil-rock mixture by large scale direct shear test. Int J Rock Mech Min Sci 48(8):1235–1247
46. Xu WJ, Yue ZQ, Hu RL (2008) Study on the mesostructure and mesomechanical characteristics of the soil-rock mixture using digital image processing based finite element method. Int J Rock Mech Min Sci 45(5):749–762
47. Yang H, Zhou Z, Wang X, Zhang Q (2015) Elastic modulus calculation model of a soil-rock mixture at normal or freezing temperature based on micromechanics approach. Adv Mater Sci Eng. https://doi.org/10.1155/2015/576080
48. Zhang HY, Xu WJ, Yu YZ (2016) Triaxial tests of soil–rock mixtures with different rock block distributions. Soils Found 56(1):44–56
49. Zhang ZL, Xu WJ, Xia W, Zhang HY (2016) Large-scale in situ test for mechanical characterization of soil-rock mixture used in an embankment dam. Int J Rock Mech Min Sci 86:317–322
50. Zhang H, Hu X, Boldini D, He C, Liu C, Ai C (2020) Evaluation of the shear strength parameters of a compacted S-RM fill using improved 2-D and 3-D limit equilibrium methods. Eng Geol. https://doi.org/10.1016/j.enggeo.2020.105550
51. Zhou Z, Yang H, Wang X, Liu B (2016) Model development and experimental verification for permeability coefficient of soil-rock mixture. Int J Geomech 17(4):04016106
52. Zhou W, Wu W, Ma G, Ng TT, Chang X (2018) Undrained behavior of binary granular mixtures with different fines contents. Powder Technol 340:139–153